The International Journal of Advanced Manufacturing Technology (2022) 120:3669–3681
https://doi.org/10.1007/s00170-022-08994-8

ORIGINAL ARTICLE

Multi-objective process parameters optimization in rapid heat cycle molding incorporating variable packing pressure profile for improving weldline, clamping force, and cycle time

Satoshi Kitayama[1] · Shogo Tsurita[2] · Masahiro Takano[3] · Yusuke Yamazaki[4] · Yoshikazu Kubo[4] · Shuji Aiba[4]

Received: 21 December 2021 / Accepted: 26 February 2022 / Published online: 7 March 2022

Abstract
Rapid heat cycle molding (RHCM) that actively controls the mold temperature has attracted attention in plastic injection molding (PIM) for improving product surface quality. In the RHCM, the mold temperature profile plays a crucial role for producing products with high surface quality, but the profile as well as other process parameters is determined by the trial-and-error method. In this paper, weldline, clamping force, and cycle time are simultaneously minimized for the high product quality and the high productivity using the RHCM. The RHCM generally requires cycle time long, and then variable packing pressure profile that the packing pressure varies during PIM process is adopted to shorten the cycle time. The numerical simulation in the RHCM is computationally so expensive that sequential approximate optimization using radial basis function network is adopted to determine the optimal process parameters, and the pareto-frontier among weldline, clamping force and cycle time is identified. It is found from the numerical result that the optimal pressure profiles start with the low packing pressure and the high packing pressure is applied at the end of packing phase. The mold temperature increases due to the high packing pressure, and the high mold temperature makes the flow of melt plastic smooth. Consequently, the weldline reduction can be achieved. Based on the numerical result, the experiment using the PIM machine (MS100, Sodick) is carried out. Compared to the conventional PIM, the weldline reduction can be achieved with smaller clamping force.

Keywords Rapid heat cycle molding · Plastic injection molding · Weldline · Clamping force · Sequential approximate optimization

1 Introduction

Plastic injection molding (PIM) is an industrial manufacturing technology to produce plastic products. Plastic products have several good properties such as lightweight, high gloss appearance, high corrosion resistance and low cost with high productivity, and cellular phone cover or decorative components of automotive is produced by the PIM [1, 2]. The conventional PIM consists of three phases: the filling phase that the melt plastic is filled into the die cavity, the packing phase that the melt plastic is packed with a high packing pressure for the desirable shape, and the cooling phase

✉ Satoshi Kitayama
kitayama-s@se.kanazawa-u.ac.jp

Shogo Tsurita
stsurita@stu.kanazawa-u.ac.jp

Masahiro Takano
takano@irii.jp

Yusuke Yamazaki
yamazaki-y@sodick.co.jp

Yoshikazu Kubo
kuboy@sodick.co.jp

Shuji Aiba
aibas@sodick.co.jp

[1] Kanazawa University, Kakuma-machi, Kanazawa 920-1192, Japan

[2] Graduate School of Natural Science & Technology, Kanazawa University, Kakuma-machi, Kanazawa 920-1192, Japan

[3] Industrial Research Institute of Ishikawa, 2-1, Kuratsuki, Kanazawa 920-8203, Japan

[4] Sodick Co., Ltd, Ka-1-1, Miya-machi, Kaga-shi, Ishikawa 922-0595, Japan

that the melt plastic is cooled down for solidification. On the other hand, there are several defects in plastic products such as warpage, volume shrinkage, weldlines, short shot, and flash. It is well known that the process parameters such as mold temperature, melt temperature, injection pressure, injection time, packing pressure, packing time, and cooling time have an influence on these defects, and the process parameters are then adjusted through the experiment or engineering experience for high product quality and high productivity. Recently, computer aided engineering (CAE) coupled with design optimization has been recognized as one of the effective tools available to determine the process parameters. Numerical simulation in the PIM is computationally so expensive that response surface or sequential approximate optimization (SAO) that the response surface is repeatedly constructed and optimized is a major approach for the process parameters optimization [3]. In this paper, rapid heat cycle molding (RHCM) that actively controls the mold temperature is adopted as the PIM, and variable packing pressure profile that the packing pressure varies during the packing phase is used. Many papers for the process parameters optimization in PIM have been published and it is difficult to review all of them. Then, the related papers are briefly reviewed below.

First, the papers on PIM using variable packing pressure profile are reviewed. Gao and Wang adopted the Kriging in order to determine the variable packing pressure profile [4], in which warpage of a cellular phone cover was minimized. Li et al. optimized the variable packing pressure profile for achieving the shrinkage evenness of a rectangular slab [5], in which radial basis function (RBF) was used to construct the response surface of objective function, unlike Gao and Wang [4]. These papers mainly focused on the variable packing pressure profile, which were optimized. Kitayama et al. adopted the variable packing pressure profile for warpage reduction of a food tray [6], in which not only the variable packing pressure profile but also other process parameters such as the melt temperature, the mold temperature and the injection time were optimized using sequential approximate optimization with the RBF network [7]. In above papers, the validity of the variable packing pressure profile was examined through the numerical simulation using Moldflow or Moldex3D, and a single objective (warpage reduction) was considered. Unlike above papers, a multi-objective optimization for minimizing warpage and cycle time has been performed by Kitayama et al. [8], in which a box-type plastic product was handled and the validity of the variable packing pressure profile has been confirmed through the experiment using the PIM machine. This paper clarified the variable packing pressure profile was practicable PIM technology for high product quality and high productivity. After that, the PIM using variable packing pressure profile is recognized as one of the effective approaches for high product quality, and similar approach has been reported in Feng and Zhou [9, 10], in which weldline, shrinkage, and warpage of an air-conditioner vent were simultaneously minimized, or warpage, shrinkage, and sink marks of a plastic gear were minimized. It is found from the above brief review on variable packing pressure that the approach is mainly used for the high product quality such as warpage reduction.

Next, the RHCM is considered. Figure 1 shows a schematic mold temperature profile, in which T_g, denote the glass transition temperature of a material. T_H and T_L denote a heat and cool temperature, respectively. t_h,t_{inj}, t_p, and t_c denote the heating time, the injection, the packing, and the cooling time, respectively. In the RHCM, the mold is heated rapidly above the glass transition temperature before the filling phase, and the melt plastic is injected into the die cavity. After that, the mold is rapidly cooled down, and the plastic product is finally ejected. It is found from Fig. 1 that the RHCM mainly consists of four phases unlike the conventional PIM. Therefore, the heating phases are newly introduced before the filling phase. By introducing the heating phase, the melt plastic is smoothly filled into the die cavity under high mold temperature. It is expected that weldlines that are formed when two or more melt fronts meet will be diminished and the high surface quality product will then be produced.

Li et al. optimized the diameter and center coordinates of heating channel for LCD TV panel using the RHCM [11], in

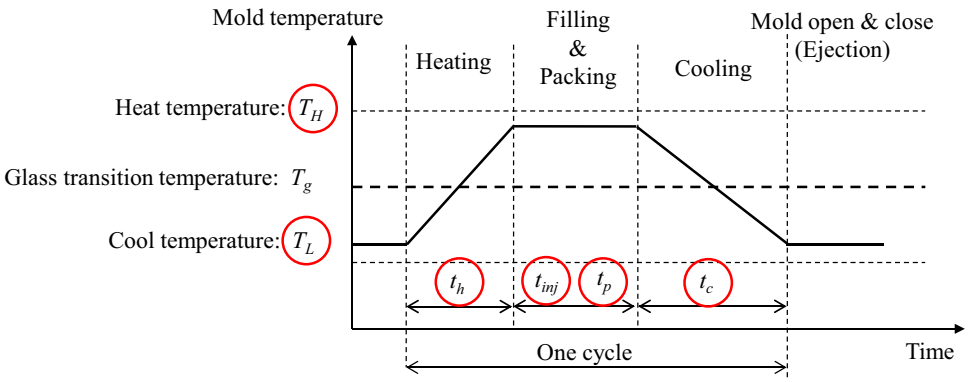

Fig. 1 Schematic mold temperature profile in rapid heat cycle molding

which the average mold temperature was maximized for the heating efficiency, whereas the mold temperature distribution was minimized for the uniform temperature distribution. Therefore, the multi-objective optimization was formulated to determine the optimal diameter and center coordinates of heating channel. The multi-objective genetic algorithm (MOGA) was used to identify the pareto-frontier. Wang et al. optimized the layout of heating/cooling channels of a mold in the RHCM [12], in which the heating time, the mold temperature distribution and the von Mises stress of the mold were considered. Like Li et al. [11], the diameter and the center coordinates of channels were taken as the design variables. The heating time was minimized for heating efficiency under the design constraints of the mold temperature and the von Mises stress. Wang et al. also optimized the layout of cooling channels of a mold in the RHCM [13], in which both the heating time and the mold temperature were minimized for the heating efficiency and the uniform temperature distribution. Second-order polynomial was used for the response surface of objective functions, and the diameter and the center coordinates of channels were then optimized. The layout optimization of heating/cooling channels has also been conducted in Xiao and Huang [14]. The basic idea of RHCM was extended to glass molding process (GMP) and was successfully applied [15]. It is found from the above brief review that one of the major topics in the RHCM is the layout optimization of heating/cooling channels, and the process parameters including the mold temperature profile are rarely discussed in the literature. However, the mold temperature profile as well as the process parameters in the RHCM has strongly an influence on the product quality and the productivity, and it is then important to optimize the mold temperature profile and other process parameters for high product quality and high productivity.

Due to the advancement of 3D printing technology, it is possible to fabricate conformal cooling channels that greatly influence on the cooling performance. Xu et al. investigated the mold temperature histories between the straight and the conformal cooling channel [16], from which it was clarified that the conformal cooling channel could quickly reach to the steady state condition. This suggests that the conformal cooling channel will be suitable to the RHCM that controls the mold temperature quickly. Dimla et al. conducted the finite element analysis (FEA) and the thermal heat transfer analysis of conformal cooling channel [17], in which the temperature behavior and the position of cooling channel in the core and cavity were investigated and they suggested that the cooling time would be reduced, compared to the traditional straight line-drilled cooling channel. After that, Au and Yu proposed a design method for conformal cooling channel and applied it to blow molding [18], from which it was clarified that the cooling time could be reduced, compared to the traditional straight line-drilled cooling channel through the numerical simulation. Kitayama et al. performed the process parameters optimization for minimizing warpage and cycle time [19], in which the superiority of conformal cooling channel was numerically and experimentally clarified, compared to the straight line-drilled cooling channel. Zhang et al. optimized several process parameters so as to minimize warpage and clamping force [20], in which a conformal cooling channel was also adopted to improve the temperature distribution. It was reported from the numerical result that the clamping force as well as the warpage was well improved, compared to a conventional cooling channel. Kuo et al. and Kuo and Chen developed conformal cooling channels for wax injection molding and hot embossing stamping using additive manufacturing technology [21, 22]. Kuo et al. also investigated the optimal distance between the wall of conformal cooling channel and the surface of injection mold [23].

Shayfull et al. pointed out [24] that the cooling performance would be drastically improved when conformal cooling channel for uniform heating/cooling was used to the RHCM. Kirchheim et al. fabricated the conformal cooling channel by a metal 3D printer and the RHCM was experimentally conducted [30], from which it was found that both the cycle time and the product surface quality could be improved. However, the process parameters in the RHCM were not clearly described. Due to the high mold temperature during the heating phase, the long cooling time is generally required, which makes the productivity low. For high productivity, it is important to shorten the cycle time in the RHCM as much as possible.

Here, our objectives of this paper are summarized as follows:

1. The RHCM is used for high product quality and high productivity. In this paper, weldline is considered as the product surface quality, and is minimized. Based on Kitayama et al. [25], the mold temperature during the heating phase is maximized for weldline reduction.
2. High mold temperature during the heating phase makes the cycle time long. On the other hand, as described above, the variable packing profile is valid to short cycle time. Then, the variable packing pressure profile is adopted to shorten the cycle time in the RHCM. However, it is difficult to determine the mold temperature profile as well as the variable packing pressure profile. To determine them, design optimization using numerical simulation of RHCM is performed in this paper.
3. Clamping force plays an important role in the PIM for energy consumption [26]. It is much preferable to produce plastic product with a small energy consumption for green environment. Zhang et al. determined the optimal process parameters so as to minimize the warpage and the clamping of a plastic oil cooler cover of diesel engine [20],

and Kitayama and Natsume also optimized the process parameters so as to minimize the volume shrinkage and the clamping force of a plastic cap [27]. Clamping force has a direct influence on the scale of PIM machine. Therefore, it is possible to produce plastic product with a small-scale PIM machine when the clamping force is small. On the other hand, a large-scale PIM machine is required to produce plastic product with large clamping force. It is important to minimize the clamping force as much as possible for high productivity as well as high product quality.

In this paper, a multi-objective process parameters optimization in the RHCM incorporating variable packing pressure profile is performed, in which three objective functions (the mold temperature, the clamping force and the cycle time) are considered. Considering the suggestion by Shayfull et al. [24], conformal cooling channel that is uniformly heated and cooled is used. The numerical simulation in PIM is computationally so expensive that sequential approximate optimization using radial basis function network is adopted to identity the pareto-frontier among three objectives [7].

The rest of this paper is organized as follows: in Sect. 2, the numerical simulation model with the conformal cooling channel is described. In Sect. 3, the multi-objective optimization is explained. The numerical result is shown in Sect. 4. Based on the numerical result, the experiment using PIM machine (MS100, Sodick) is carried out to examine the validity of the proposed approach. Moldex3D-2020is used for the PIM numerical simulation.

2 Numerical simulation model and RHCM simulation

Figure 2 shows the target plastic product with the conformal cooling channel handled in this paper, in which Fig. 2b shows the numerical simulation model with the dimensions. The side wall thickness is 0.35 mm and the width is 20.6 mm. The overview of conformal cooling channel and the enlarged view enclosed by black circle are shown in Fig. 2c, where the diameter of cooling channel is 8 mm. Acrylonitrile–butadiene–styrene (ABS) is used as the material and the property taken from the database of Moldex3D is listed in Table 1. Figure 3 shows the flow process, in which the melt plastic is injected from the gate and flows into the side wall (Fig. 3a). Then, the flow front meets around the center of side wall (Fig. 3b) and the weldline is generated (Fig. 3c).

Next, the RHCM simulation using Moldex3D is explained. As described in Sect. 1, the RHCM consists of four phases: the heating, the filling, the packing, and the cooling phase. In this paper, water flowing into the conformal cooling channel is used as the coolant, and the RHCM

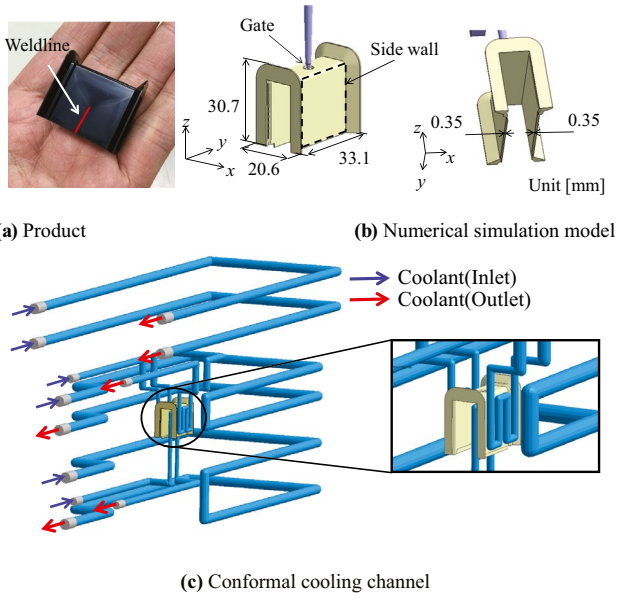

Fig. 2 Thin-walled plastic product and conformal cooling channel

simulation is conducted by controlling the water temperature flowing into the channel. The water set above the glass transition temperature is flowed into the cooling channel in the heating phase. In the cooling phase, the water set below the glass transition temperature is flowed into the cooling channel and the mold temperature is cooled down.

3 Multi-objective process parameters optimization in RHCM incorporating variable packing pressure profile

3.1 Multi-objective optimization

A multi-objective optimization problem is generally formulated as follows [28]:

$$\left.\begin{array}{l}(f_1(\mathbf{x}), f_2(\mathbf{x}), \cdots, f_K(\mathbf{x})) \rightarrow \min \\ \mathbf{x} \in X\end{array}\right\} \tag{1}$$

where $f_i(\boldsymbol{x})$ is the ith objective function to be minimized, K represents the number of objective functions. When the jth objective function $f_j(\boldsymbol{x})$ is to be maximized, it is equivalent to minimize the function $-f_j(\boldsymbol{x})$. $\mathbf{x} = (x_1, x_2, \cdots, x_n)^T$ denotes

Table 1 Material property of acrylonitrile–butadiene–styrene

Density (g/cm^3)	1.04
Eject temperature (°C)	1.09
Elastic module [GPa]	2.45
Poisson ratio	0.4
Material characteristics	Amorpous resin
Glass transition temperature (°C)	129

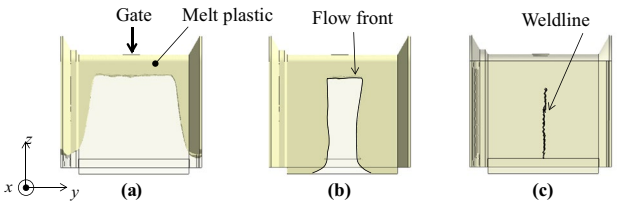

Fig. 3 Flow process and weldline of target product

the design variables, n represents the number of design variables, and X denotes the feasible region.

3.2 Design variables

As shown in Fig. 1, the mold temperature profile is completely determined by six process parameters (T_H, T_L, t_h, t_{inj}, t_p, and t_c), which are taken as the design variables. Next, the variable packing pressure profile in Fig. 4 is explained, in which the solid line represents the variable packing pressure profile and the dashed line represents the constant one. It is assumed that the profile will linearly vary during the packing phase. Therefore, the profile consists of four process parameters (P_1, P_2, $t_p{}^1$, and $t_p{}^2$). Note that the packing time (t_p) is given as $t_p = t_p^1 + t_p^2$. In addition, the melt temperature (T_{melt}) affecting the flow of melt plastic is taken as the design variables. Then, the design variables $\boldsymbol{x}$ is given by Eq. (2).

$$\mathbf{x} = (T_H, T_L, t_h, t_{inj}, t_p^1, t_p^2, t_c, P_1, P_2, T_{melt})^T \tag{2}$$

The lower and upper bounds of the design variables are also given by Eq. (3).

$$\left.\begin{array}{l} 220 \le T_{melt}[^\circ C] \le 260 \;\; 135 \le T_H[^\circ C] \le 170 \;\; 40 \le T_L[^\circ C] \le 70 \\ 10 \le t_h[s] \le 50 \;\; 0.1 \le t_{inj}[s] \le 1.0 \;\; 5.0 \le t_p^1[s] \le 10 \;\; 10 \le t_p^2[s] \le 15 \\ 25 \le t_c[s] \le 40 \;\; 50 \le P_1[MPa] \le 80 \;\; 50 \le P_2[MPa] \le 80 \end{array}\right\} \tag{3}$$

The lower bound of T_H is set above the glass transition temperature, whereas the upper bound of T_H is set considering the experimental condition. The range of t_h and t_c are determined by considering the heat/cool temperature controller in the experiment. The range of t_p is determined by considering the gate seal time. The mold will be damaged when the packing pressure of 80 MPa is applied, and the upper bound of P_1 and P_2 is set to 80 MPa. Finally, the recommended value in Moldex3D is used for T_L, T_{melt}, and t_{inj}.

3.3 Objective functions

In this paper, three objective functions (weldline, clamping force, and cycle time) are simultaneously minimized for high product quality and high productivity. Based on Kitayama et al. [25], the mold temperature during the heating phase in RHCM is maximized for the weldline reduction.

Here, the relation among the three objectives is shown in Fig. 5. First, the relation between weldline and cycle time in the RHCM is considered. As reported in Refs [12, 14, 24, 25], the higher mold temperature is, the shorter weldline is. However, the high mold temperature makes the cooling time long, and consequently the long cycle time is required. On the other hand, it is possible to produce the product with short cycle time when the mold temperature is low. However, in this case, the weldline is long. Therefore, the trade-off between them is observed.

Next, the relation between weldline and clamping force is discussed. Kitayama et al. investigated the relation between the weldline and the clamping force [29], in which it was reported through the numerical and experimental result that the larger the clamping force was, the shorter the weldline was. However, the relation between them is rarely discussed in the literature.

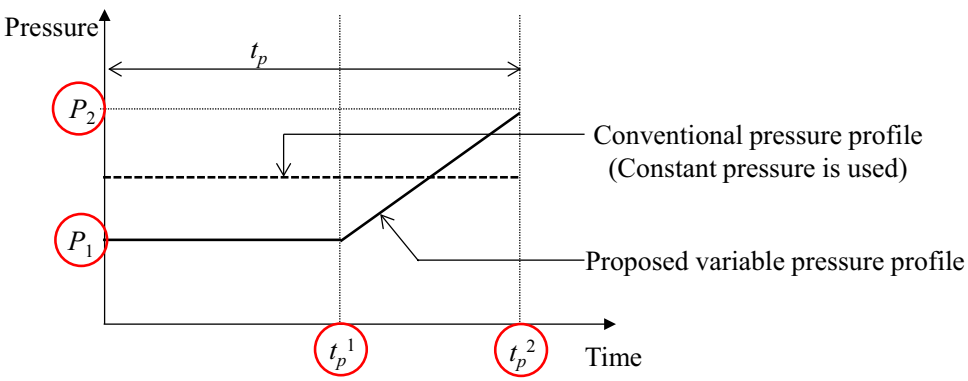

Fig. 4 Design variables for variable packing pressure profile

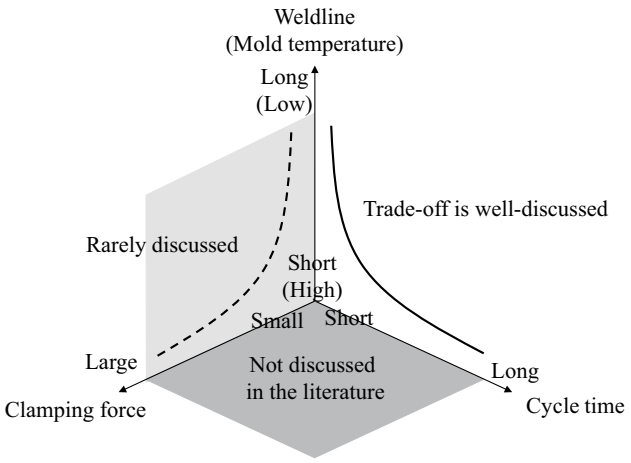

Fig. 5 Relation among weldline, clamping force, and cycle time

Finally, the relation between clamping force and cycle time is considered. As far as we survey, the relation between the clamping force and the cycle time is not discussed in the literature. As described in introduction, clamping force will be so closely related to product quality as well as productivity. On the other hand, high productivity is always required in the PIM. Therefore, it is important to discuss the relation between the clamping force and the cycle time.

The first objective function $f_1(\boldsymbol{x})$ that is the mold temperature T_{mold} during the heating phase is maximized for weldline reduction. Therefore, $f_1(\boldsymbol{x})$ is given by Eq. (4).

$$f_1(\mathbf{x}) = -T_{mold} \rightarrow \min \tag{4}$$

The clamping force is taken as the second objective function $f_2(\boldsymbol{x})$ to be minimized for high product quality and high productivity. The cycle time is considered as the third objective function $f_3(\boldsymbol{x})$ to be minimized for high productivity. $f_3(\boldsymbol{x})$ is given by Eq. (5) as the explicit form of the design variables.

$$f_3(\mathbf{x}) = t_h + t_{inj} + t_p^1 + t_p^2 + t_c \rightarrow \min \tag{5}$$

Note that the mold temperature and the clamping force are numerically evaluated through the computationally expensive RHCM simulation.

3.4 Sequential approximate optimization

The numerical procedure to identify the pareto-frontier using the SAO using RBF network is briefly described in this section. See Kitayama et al. [7] for the detail of the RBF network.

(Step 1) The Latin hypercube design (LHD) is used to generate some initial sampling points (LHD). Therefore, several combinations of the process parameters are determined.

(Step 2) The numerical simulation using Moldex3D is carried out. Then, three objective functions are numerically evaluated.

(Step 3) All functions are approximated by the RBF network. Here, the approximated objective functions are denoted as $\tilde{f}_k(\mathbf{x})(k = 1, 2, 3)$.

(Step 4) The pareto-optimal solutions are determined by using the weighted lp norm method formulated as follows:

$$\left.\begin{array}{l} \left[\sum_{k=1}^{3} \left(\alpha_k \tilde{f}_k(\mathbf{x})\right)^p\right]^{1/p} \rightarrow \min \\ x_i^L \le x_i \le x_i^U \;\; i = 1, 2, , n \end{array}\right\} \tag{6}$$

where $\alpha_k(k = 1, 2, 3)$ represents the weight of the k-th objective function under the following condition.

$$\alpha_1 + \alpha_2 + \alpha_3 = 1 \tag{7}$$

p in Eq. (6) is the parameter. According to Kitayama et al. [8, 19, 25, 29], p is set to 4. In order to obtain a set of pareto-optimal solutions, various weights are assigned.

(Step 5) If a terminal criterion is satisfied, the SAO algorithm will terminate. Otherwise, the pareto-optimal solutions in STEP4 are added as the new sampling points for improving the accuracy of pareto-frontier. As the result, the number of sampling points is updated. Then, return to Step 2.

The average error between the response surface and the numerical simulation at the pareto-optimal solutions is taken as the terminal criterion. The SAO algorithm will terminate when the average error is within 5%. The algorithm is shown in Fig. 6.

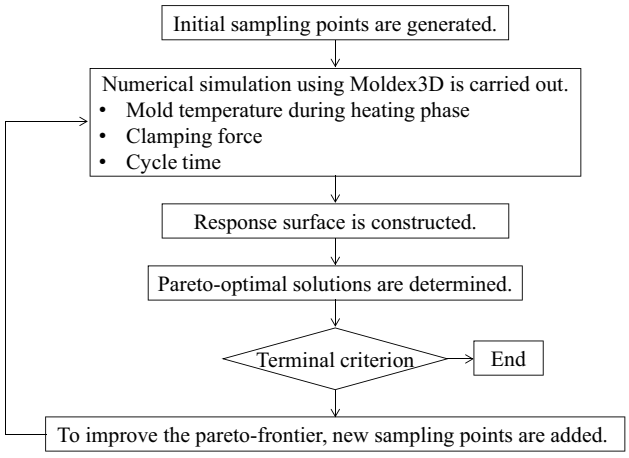

Fig. 6 Sequential approximate optimization algorithm to identify pareto-frontier

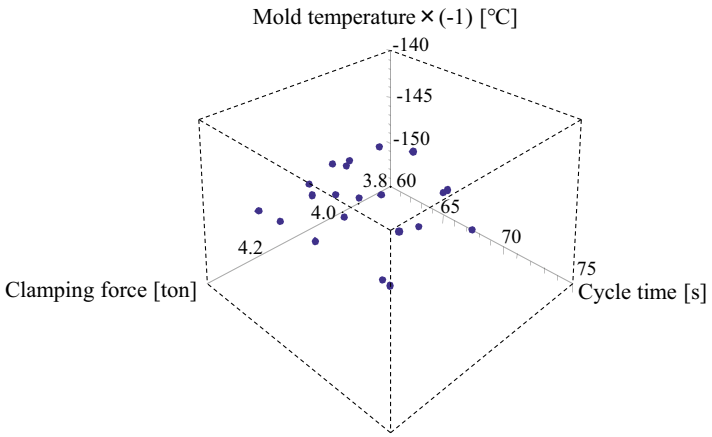

(a) Pareto-frontier among three objectives

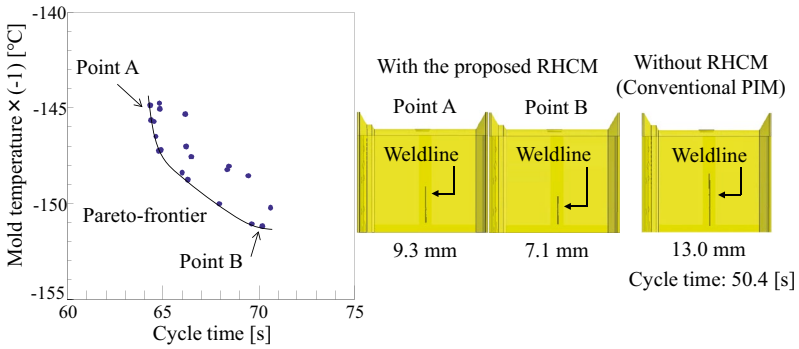

(b) Pareto-frontier between cycle time and mold temperature

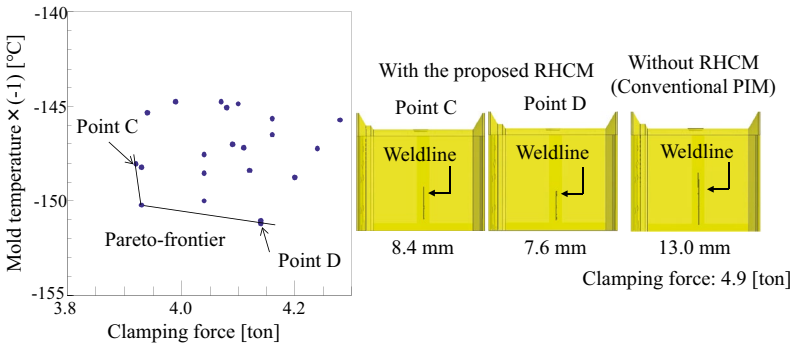

(c) Pareto-frontier between mold temperature and clamping force

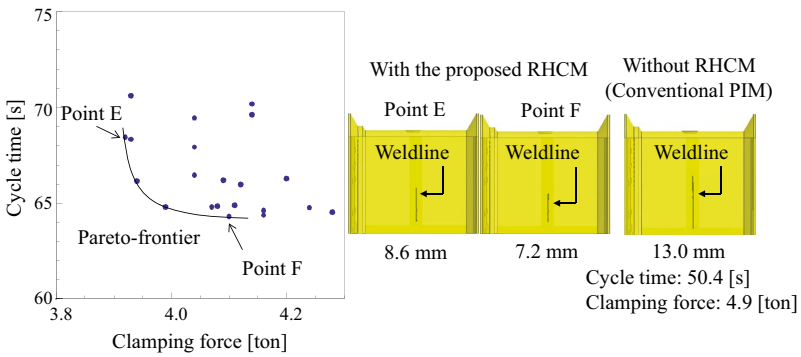

(d) Pareto-frontier between clamping force and cycle time

Fig. 7 Pareto-optimal solutions of RHCM using variable packing pressure profile. **a** Pareto-frontier among three objectives. **b** Pareto-frontier between cycle time and mold temperature. **c** Pareto-frontier between mold temperature and clamping force. **d** Pareto-frontier between clamping force and cycle time

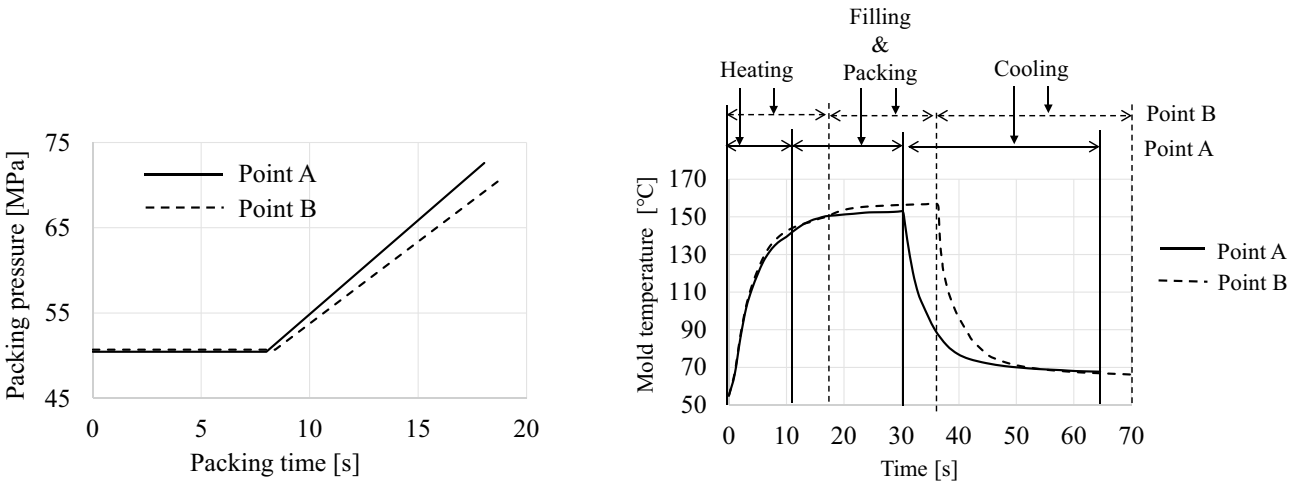

(a) Optimal variable packing pressure profile

(b) Mold temperature profile

Fig. 8 Optimal variable packing pressure profile and mold temperature profile at points A and B. **a** Optimal variable packing pressure profile. **b** Mold temperature profile

4 Numerical and experimental result

4.1 Numerical result

Twenty-five initial sampling points are generated by the LHD, and the pareto-frontier among the three objective functions is identified. Note that there is no clear criterion about the number of initial sampling points using the LHD. Considering the number of design variables, the number of initial sampling points is determined by our engineering experience. Figure 7a shows the pareto-optimal solutions with the black dots. To identify the pareto-frontier, 89 simulations are required. The relation between the cycle time and the mold temperature, between the mold temperature and the clamping force, and between the clamping force and the cycle time is shown in Fig. 7b–d, in which the solid line denotes the pareto-frontier. The weldline length at points A, B, C, D, E, and F is also shown in the figure. Note that -1 is multiplied to the axis of mold temperature (see Fig. 5). For the comparison, the weldline using the conventional PIM is shown in the figure. The cycle time and the clamping force by the conventional PIM is 50.4 s and 4.9 ton, respectively. It is found from Fig. 7b–d that the weldline and the clamping force are well reduced, compared to the conventional PIM. On the other hand, the cycle time by the conventional PIM is 50.4 s, which implies that the cycle time of RHCM is not improved.

First, Fig. 7b is considered, from which it is found that the higher the mold temperature is, the shorter the weldline is. However, the long cycle time is required, and consequently the trade-off between is observed. It is considered that the melt plastic is smoothly injected into the cavity with the high mold temperature, and the weldline is consequently reduced.

Next, Fig. 7c is considered, from which it is found that the higher the clamping force is, the higher the mold temperature is. This result indicates that weldline is reduced with the high clamping force by the proposed RHCM.

Finally, Fig. 7d is discussed, from which it is found that the shorter the cycle time is, the higher the clamping force is. In addition, the weldline at point F is shorter than that at point E. This result indicates that the clamping force plays an important role for improving the cycle time as well as the weldline reduction in the proposed RHCM. Compared to the conventional PIM, the clamping force of 20% can be reduced at point E.

Next, the optimal variable packing pressure profile is shown in Fig. 8a. Two points (points A and B) in Fig. 7b are selected for the comparison. It is found from Fig. 8a that both optimal pressure profiles start with the low packing pressure and the high packing pressure is applied at the end of packing phase. The difference of variable packing pressure profile between two points is not clear, but the cycle time is different due to the heating time. The heating time at point A is 11.0 s, whereas the one at point B is 17.7 [s]. The high mold temperature (145 [$^{\circ}C$] at point A and 151 [$^{\circ}C$] at point B) results in the long cycle time. The mold temperature profile at points A and B is also shown in Fig. 8b, from which it is found that the longer the heating time is, the longer the cycle time is. The mold temperature during the filling and packing phase increases due to the high packing pressure at the end of packing phase. The high mold temperature during the filling and packing phase makes the flow of melt plastic smooth, and the weldline can be reduced.

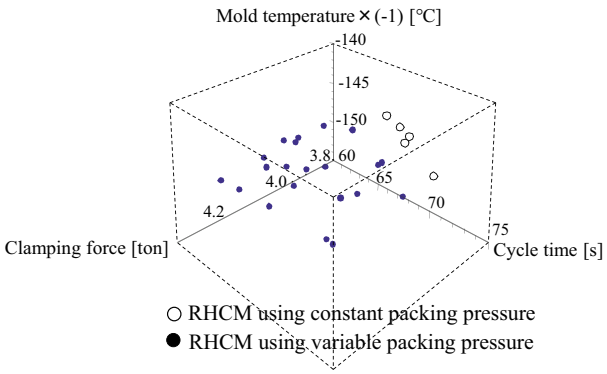

(a) Pareto-optimal solutions among three objectives

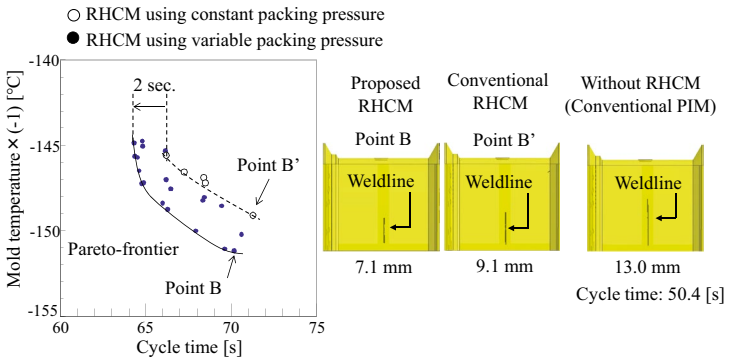

(b) Pareto-frontier between cycle time mold temperature

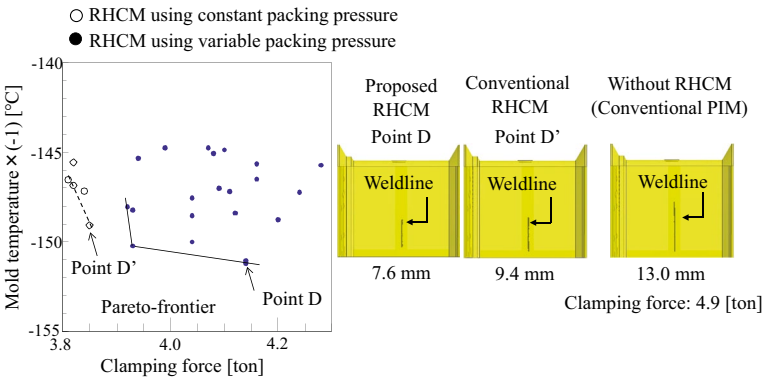

(c) Pareto-frontier between mold temperature and clamping force

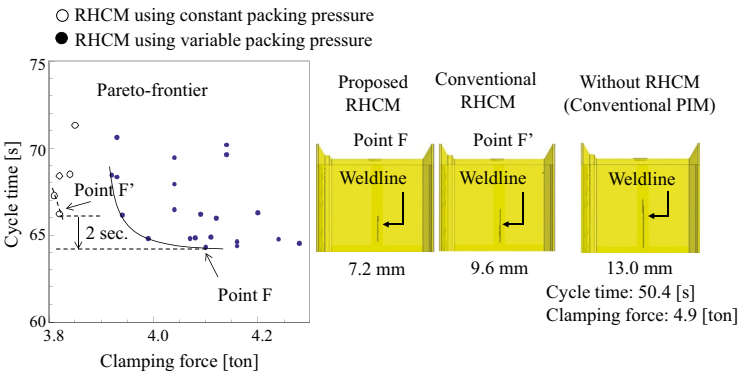

(d) Pareto-frontier between clamping force and cycle time

Fig. 9 Pareto-optimal solutions using conventional RHCM (white dots). **a** Pareto-optimal solutions among three objectives. **b** Pareto-frontier between cycle time mold temperature. **c** Pareto-frontier between mold temperature and clamping force. **d** Pareto-frontier between clamping force and cycle time

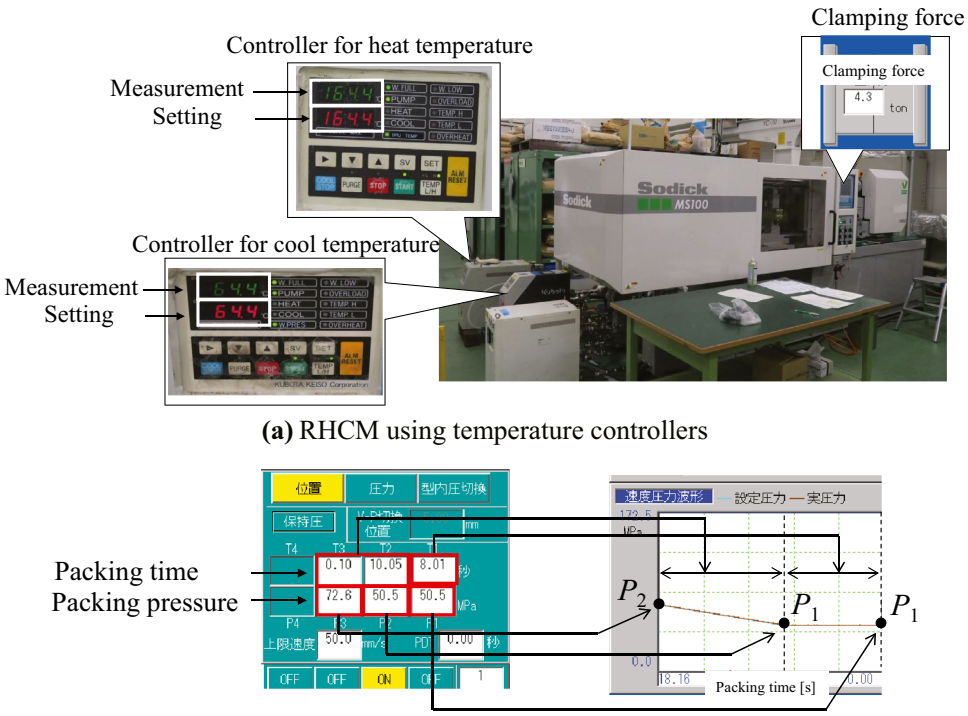

Fig. 10 Experiment of RHCM using PIM machine (MS100, Sodick). **a** RHCM using temperature controllers. **b** Variable packing pressure profile at point A in the experiment

4.2 Comparison to conventional RHCM using constant packing pressure

The RHCM using a constant packing pressure during the packing phase is used for the comparison of the proposed RHCM. The mold temperature profile and other process parameters are optimized by the method described in Sect. 3.4. The process parameters (T_H, T_L, t_h, t_{inj}, t_p, and t_c) in Fig. 1 are taken as the design variables. In addition, the packing pressure P and the melt temperature T_{melt} are taken as the design variables. The lower and upper bounds of the design variables are given by Eq. (8).

$$\left.\begin{array}{l} 220 \le T_{melt}[^\circ C] \le 260 \;\; 135 \le T_H[^\circ C] \le 170 \;\; 40 \le T_L[^\circ C] \le 70 \\ 10 \le t_h[s] \le 50 \;\; 0.1 \le t_{inj}[s] \le 1.0 \;\; 15 \le t_p[s] \le 25 \;\; 25 \le t_c[s] \le 40 \\ 50 \le P[MPa] \le 80 \end{array}\right\} \tag{8}$$

Like Sect. 4.1, 25 initial sampling points are generated by the LHD, and the pareto-frontier is identified. Ninety simulations are required to identify the pareto-frontier. The pareto-frontier among the three objectives is shown in Fig. 9a, in which the black dots denote the pareto-optimal solutions by the proposed RHCM and the white dots denote the ones by the conventional RHCM. It is found from Fig. 9a that the pareto-optimal solutions by the conventional RHCM are not well distributed, compared to the ones by the proposed RHCM.

Like Fig. 7, the relation between the mold temperature and the cycle time, between the mold temperature and the clamping force, and between the clamping force and the cycle time is shown in Fig. 9b–d, in which the black dots denote the pareto-optimal solutions by the proposed RHCM and the white dots denote the ones by the conventional RHCM. The dashed line represents the pareto-frontier by the conventional RHCM. In addition, the weldline at points B', D', and F' is shown for the comparison.

It is found from Fig. 9b that the cycle time and the mold temperature are well improved by the proposed RHCM. In addition, the cycle time by the proposed RHCM is improved, compared to the one by the conventional RHCM. This result indicates that the variable packing pressure profile can improve the cycle time effectively.

Next, Fig. 9c is considered, from which it is found that the mold temperature by the proposed RHCM is higher than that by the conventional RHCM. However, the clamping force by the conventional RHCM is smaller than that by the proposed RHCM.

Table 2 Optimal process parameters at point A

T_h [°C]	t_h [s]	T_{melt} [°C]	t_{inj} [s]	P_1 [MPa]	P_2 [MPa]	t_P^1 [s]	t_P^2 [s]	T_c [°C]	t_c [s]	Mold temperature [°C]	Clamping force [ton]	Cycle time [s]
164.4	11.10	252.1	0.66	50.5	72.6	8.01	10.05	64.4	34.71	145.72	4.3	64.53

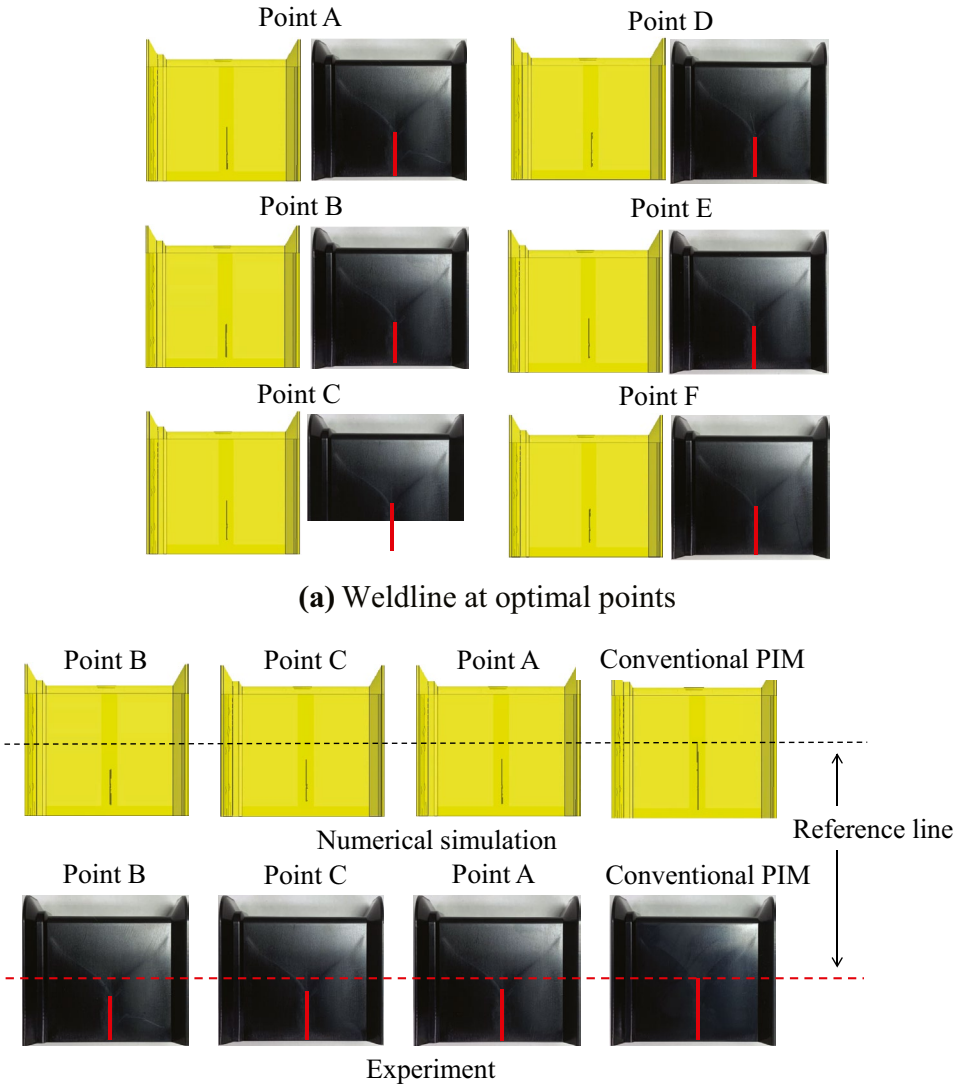

Fig. 11 Weldline in numerical simulation and experiment. **a** Weldline at optimal points. **b** Comparison of weldline length with conventional PIM

Finally, Fig. 9d is discussed. As shown in this figure, the cycle time by the proposed RHCM is shorter than that by the conventional RHCM. It is considered that the proposed RHCM is more flexible PIM technology for high product quality and high productivity than the conventional RHCM. In particular, the weldline by the proposed RHCM is shorter than that by the conventional RHCM through all points, and this result indicates that the proposed RHCM can effectively reduce the weldline and the cycle time.

4.3 Experimental result

The experiment using PIM machine in Fig. 10 (MS100, Sodick) is carried out to examine the validity of the proposed RHCM. The conformal cooling channel shown in Fig. 2c is fabricated by 3D metal printer (OPM250L, Sodick). As shown in Fig. 10a, two temperature controllers for heat and cool are equipped to conduct the RHCM. In the experiment, the clamping force is inputted in the

Table 3 Comparison of weldline length between numerical simulation and experiment

	Point A	Point B	Point C	Point D	Point E	Point F	Conventional PIM (Without RHCM)
Numerical simulation [mm]	9.3	7.1	8.4	7.6	8.6	7.2	13.0
Experiment [mm]	10.9	9.8	10.2	10.0	10.3	10.0	11.6
Error [%]	14.7	27.6	17.6	23.7	16.5	28.0	12.1

PIM machine, and the example of the controllers and the clamping force at point A in the experiment is shown in Fig. 10a. In addition, the variable packing pressure profile at point A in the experiment is shown in Fig. 10b. Note that the horizontal axis (packing time) in the experiment is in reverse, compared to the one in the numerical simulation. The optimal process parameters at the point are listed in Table 2.

The weldline at optimal points in the experiment is shown in Fig. 11a with the numerical simulation, in which the red line denotes the weldline in the experiment. The comparison of the weldline by the conventional PIM is also shown in Fig. 11b, in which the dashed line denotes the reference line for the comparison. It is found from Fig. 11b that the weldline by the proposed RHCM is shorter than that by the conventional PIM. The weldline length is also listed in Table 3, from which the error is slightly large. Since the PIM machine is accurately controlled, it is considered that one of the major factors for the error is the variation of the material property. The variation of material property is an uncontrollable parameter in the experiment. To obtain more accurate result, it is important to perform a robust design optimization considering the variation of material property or process parameters [31, 32].

5 Conclusion

RHCM is recognized as one of the important manufacturing technologies to produce plastic product with high surface quality, but the mold temperature profile as well as the other process parameters is determined by the trial-and-error method. In addition, the RHCM generally requires a long cooling time due to the high mold temperature. The variable packing pressure profile is recognized as one of the effective PIM technologies for high productivity, but it is difficult to determine the process parameters in advance. To determine the optimal process parameters in the RHCM incorporating the variable packing pressure profile, design optimization for minimizing weldine, clamping force, and cycle time was performed. Numerical simulation in the RHCM was so intensive that sequential approximate optimization using radial basis function network was adopted to identify the pareto-frontier. The conventional RHCM was also investigated to compare the weldline by the proposed RHCM. As the result, the trade-off between the clamping force and the cycle time was clarified by the proposed RHCM. It was impossible to improve the cycle time by the proposed RHCM, compared to the one by the conventional PIM. However, the clamping force of 20% could successfully be reduced. Finally, to examine the validity of the proposed RHCM, the experiment using the PIM machine (MS100, Sodick) was conducted. Through the numerical and experimental result, it was clarified that the weldline reduction could be achieved by the proposed RHCM.

Authors' contributions All authors have contributed to this research. All authors read and approved the final manuscript.

Funding This research is partially supported by Grants-in-Aided for Scientific Research from Japan Society for the Promotion of Science (JSPS).

Availability of data and materials The data that support the findings of this study are openly available.

Declarations

Ethics approval This manuscript includes no ethical issues of life science fields.

Consent to participate I have already gotten consent of all authors to participate.

Consent for publication I have already gotten consent of all authors to publish.

Competing interests The authors declare that they have no competing interests.

References

1. Gao Y, Wang X (2008) An effective warpage optimization method in injection molding based on the Kriging model. Int J Adv Manuf Technol 37:953–960
2. Shie JR (2008) Optimization of injection molding process for contour distortions of polypropylene composite components by a radial basis neural network. Int J Adv Manuf Technol 36:1091–1103
3. Dang XP (2014) General frameworks for optimization of plastic injection molding process parameters. Simul Model Pract Theory 41:15–27
4. Gao Y, Wang X (2009) Surrogate-based process optimization for reducing warpage in injection molding. J Mater Process Technol 209:1302–1309
5. Li C, Wang FL, Chang YQ, Liu Y (2010) A modified global optimization method based on surrogate model and its application in packing profile optimization of injection molding process. Int J Adv Manuf Technol 48:505–511
6. Kitayama S, Onuki R, Yamazaki K (2014) Warpage reduction with variable pressure profile in plastic injection molding via sequential approximate optimization. Int J Adv Manuf Technol 72:827–838
7. Kitayama S, Arakawa M, Yamazaki K (2011) Sequential approximate optimization using radial basis function network for engineering optimization. Optim Eng 12:535–557
8. Kitayama S, Yokoyama M, Takano M, Aiba S (2017) Multi-objective optimization of variable packing pressure profile and process parameters in plastic injection molding for minimizing warpage and cycle time. Int J Adv Manuf Technol 92:3991–3999
9. Feng QQ, Zhou X (2019) Automated and robust multi-objective optimal design of thin-walled product injection process based on hybrid RBF-MOGA. Int J Adv Manuf Technol 101:2217–2231

10. Alvarado-Iniesta A, Cuate O, Schutze O (2019) Multi-objective and many objective design of plastic injection molding process. Int J Adv Manuf Technol 102:3165–3180
11. Li XP, Zhao GQ, Guan YJ, Ma MX (2009) Multi-objective optimization of heating channels for rapid heating cycle injection mold using Pareto-based genetic algorithm. Polym Adv Technol 21:669–678
12. Wang G, Zhao G, Li H, Guan Y (2011) Research on optimization design of the heating/cooling channels for rapid heat cycle molding based on response surface methodology and constrained particle swarm optimization. Expert Syst Appl 38:6705–6719
13. Wang M, Dong J, Wang W, Zhou J, Dai Z, Zhuang X, Yao X (2013) Optimal design of medium channels for water-assisted rapid thermal cycle mold using multi-objective evolutionary algorithm and multi-attribute decision-making method. Int J Adv Manuf Technol 68:2407–2417
14. Xiao CL, Huang HX (2014) Optimal design of heating system for rapid thermal cycling mold using particle swarm optimization and finite element method. Appl Therm Eng 64:462–470
15. Ming W, Chen Z, Du J, Zhang Z, Zhang G, He W, Ma J, Shen F (2020) A comprehensive review of theory and technology of glass molding process. Int J Adv Manuf Technol 107:2671–2706
16. Xu X, Sachs E, Allen S (2001) The design of conformal cooling channels in injection molding tooling. Polym Eng Sci 41:1265–1279
17. Dimla DE, Camilott M, Miani F (2005) Design and optimisation of conformal cooling channels in injection moulding tools. J Mater Process Technol 164–165:1294–1300
18. Au KM, Yu KM (2013) Conformal cooling channel design and CAE simulation for rapid blow mould. Int J Adv Manuf Technol 66:311–324
19. Kitayama S, Miyakawa H, Takano M, Aiba S (2017) Multi-objective optimization of injection molding process parameters for short cycle time and warpage reduction using conformal cooling channel. Int J Adv Manuf Technol 88:1735–1744
20. Zhang J, Wang J, Lin J, Guo Q, Chen K, Ma L (2016) Multiobjective optimization of injection molding process parameters based on Opt LHD. EBFNN, and MOPSO. Int J Adv Manuf Technol 85:2857–2872
21. Kuo CC, Chen WH, Liu XZ, Liao YL, Chen WJ, Huang BY, Tsai RL (2017) Development of a low-cost wax injectin mold with high cooling efficiency. Int J Adv Manuf Technol 93:2081–2088
22. Kuo CC, Chen BC (2017) Development of hot embossing stamps with conformal cooling channels for microreplication. Int J Adv Manuf Technol 88:2603–2608
23. Kuo CC, Jian ZF, Lee JH (2019) Effects of cooling time of mold parts on rapid injection molds with different layouts and surface roughness of conformal cooling channels. Int J Adv Manuf Technol 103:2169–2182
24. Shayfull Z, Sharif S, Zain AM, Ghazali MF, Saad RM (2014) Potential of conformal cooling channel in rapid heat cycle molding: a review. Adv Polym Technol 33(1). https://doi.org/10.1002/adv.21381
25. Kitayama S, Ishizuki R, Takano M, Kubo Y, Aiba S (2019) Optimization of mold temperature profile and process parameters for weld line reduction and short cycle time in rapid heat cycle molding. Int J Adv Manuf Technol 103:1735–1744
26. Yin F, Mao H, Hua L (2011) A hybrid of back propagation neural network and genetic algorithm for optimization of injection molding process parameters. Mater Des 32:3457–3464
27. Kitayama S, Natsume S (2014) Multi-objective optimization of volume shrinkage and clamping force for plastic injection molding via sequential approximate optimization. Simul Model Pract Theory 48:35–44
28. Miettinen KM (1998) Nonlinear multiobjective optimization, kluwer academic publishers
29. Kitayama S, Tamada K, Takano M, Aiba S (2018) Numerical and experimental investigation on process parameters optimization in plastic injection molding for weldlines reduction and clamping force minimization. Int J Adv Manuf Technol 97:2087–2098
30. Kirchheim A, Katrodiya Y, Zumofen L, Ehrig F, Wick C (2021) Dynamic conformal cooling improves injection molding: Hybrid molds manufactured by laser powder bed fusion. Int J Adv Manuf Technol 114:107–116
31. Park GJ, Lee TH, Hwang KH (2006) Robust design: an overview. AIAA J 44:181–191
32. Kitayama S, Yamazaki K (2014) Sequential approximate robust design optimization using radial basis function network. Int J Mech Mater Des 10:313–328